



Numerical Study About the Effect of Circular Pin Configuration in Heat Sink on Heat Transfer

Mustafa Awad Khalifah¹, Sadiq Talal Bunyan¹, Nabeh Alderoubi², Ali A. Nadhim³, Muna Sabah Kassim^{1*},
Hakim S. Sultan Aljibori⁴, Hasan Shakir Majdi⁵

¹ Mechanical Engineering Department, College of Engineering, Mustansiriyah University, Baghdad 10052, Iraq

² Design and Drafting Technology Department, Lincoln Campus, Southeast Community College, Lincoln 68521, USA

³ College of Technical Engineering, Al-Farahidi University, Bagdad 10001, Iraq

⁴ College of Engineering, University of Warith Al-Anbiyaa, Karbala 56001, Iraq

⁵ Department of Chemical Engineering and Petroleum Industries, Al-Mustaqbal University College, Hillah 51001, Iraq

Corresponding Author Email: munakassim@uomustansiriyah.edu.iq

Copyright: ©2025 The authors. This article is published by IETA and is licensed under the CC BY 4.0 license (<http://creativecommons.org/licenses/by/4.0/>).

<https://doi.org/10.18280/mmep.120107>

ABSTRACT

Received: 14 March 2024

Revised: 28 June 2024

Accepted: 5 July 2024

Available online: 25 January 2025

Keywords:

numerical simulation, CFD, thermal performance, pin fin

The main purpose of this research is to examine the effect of various circular pin arrangements in heat sinks' thermal behavior. The various pin shapes include circular pins, circular pins with circumferential grooves, circular pins with hollow, perforated circular pins, and slit circular pins with the performance of the heat dissipating examined. The study uses quantitative techniques of data analysis. The numerical simulations are made with the help of ANSYS Fluent that uses the standard k-ε turbulence model. These simulations are done in 3-D to account for the flow of heat and fluids as they occur in real life. Reynolds numbers and heat fluxes are properly chosen and explained to achieve applicability in real life conditions. From the results, it can be seen that the heat transfer performance of the heat sinks is highly dependent on different arrangements of the pin. There is also a comparison of different kinds of pins and their thermal performance – it is stated that perforated and slit circular pins deliver higher performance than simple circular pins. Comparisons of the various configurations are made from the viewpoint of heat transfer coefficient, Nusselt number, and pressure drop. In the case of forced convection, five different forms of a pin fin heat sink have been examined with Re varying from 10714.3 to 432142.86 and heat fluxes ranging from 3000 W/m² to 23000 W/m². It can therefore be ascertained that with the right modification to the pin configurations significant enhancement can be achieved in heat sinks thermal efficiency. The results that are given by this study can be used to inform the design of improved cooling systems in electronic devices. Future work should include additional experiments and the investigation of other geometrical changes for heat sink improvement.

1. INTRODUCTION

Heat sinks are the most well known method of cooling the hardware used in electronics. Thermal performance for cooling electronic devices is improved by modifying the surface of the fins, rearrangement of the fins in an industry sector, there are two types from fins likes plate fin, and pin fin can be used as a heat sink. Because of the pin fins type have smaller size while, the exposed surfaces are wider, which leads the better thermal performance. Because of a rise in heat flux densities and product scaling down, applications utilizing PIFHSs for cooling of electronics have increased dramatically during the last couple of decades.

Pin fin heat sinks are used in many cooling systems in electronics because of the high heat transfer coefficient. Several researchers have investigated into the use of pins with different shapes for heat transfer enhancement. However, a detailed comparative analysis of the number of pin

configuration like; circular pins with groove, hollow circular pin, perforated circular pin and slit circular pin is scarce. As such, this study will seek to systematically analyse these configurations with the aid of numerical simulations.

Li et al. [1] used infrared thermography to assess the performance of the thermal behavior of the HSs with maintained cooling by impingement. To test the effects of HSs type, fin height and width, impinging Reynolds number, fin tip, and the pitch between nozzles on the total thermal resistance. Khan et al. [2] created models based by analytical data for cylindrical type, staggered, in-line, (pin fin) of HSs to identify transmission of heat. These models' prediction validates previous numerical/experimental results. The staggered layout produced lower heat resistance and larger pressure drop than the in-line arrangement. In laminar forced convection, Muhammad [3] quantitatively investigated the thermal performance of PIFHSs with hexagonal shapes in comparison to rectangular, square, and circular PIFHSs. The flow of fluid

and transfer of heat were considered to be 2-D, with similar z-direction for both distribution of velocity and pressure. In addition, for both staggered and in-line layouts, hydraulic and thermal performance were compared. They found that in the type of staggered, the thermal performance is greater than that of in-line layout for all PIFHSs. Arefin [4] proposed a modified PIFHS model, The pins alteration focused on expanding the pins outward. For cylindrical shape in-line arrangement, the thermal assessments of the modified PIFHSs and pin fin were analyzed quantitatively for natural convection. Based on this analytical study, they found that the modified (pin fin) HSs will outperform the conventional one.

It has been found that grooved circular pins have higher efficiency of breaking the boundary layers and therefore the heat transfer is better. Researches said that the addition of circumferential grooves augments the surface area and intensifies the turbulence, hence improving the rates of heat rejection. Nevertheless, extensive comparisons with other configurations of the same type of structures are rather limited. Muthukumarn et al. [5] investigated experimental study on the characteristics of fluid flow and heat transfer for three different type of pin fin are horizontal grooved cylindrical, perforated, and cylindrical over an in-line configuration. The grooved cylindrical pin fin provides the greatest improvement in Nusselt number. At the higher inter fin spacing ratios, the pressure drops in case of cylindrical pin fins were lower than those of grooved cylindrical and perforated fins. Circular pins are the simplest and one of the most investigated geometries in heat sink problems. Research has shown that circular pins are in the middle of the simplicity of manufacturing and heat transfer. Nevertheless, it is suggested that their performance can be improved through alterations. Manikandan and Pachaiyappan [6] carried out numerical simulation on the properties of thermal and hydraulic for the drop-shaped with perforated PIFH in staggered arrangement. Through the results, found that there are a contrasted between the drop-shaped pin fins to the rectangular and circular forms, where the rectangular and circular pin fins were equal pressure drop properties, while the drop-shaped pin fins had a less friction factor. Anuar et al. [7] performed numerical study for processor of CPU using a program of COMSOL Multiphysics for the PIFHS thermal performance at a different in-line layout. A numerical result revealed that the changing in-line arrangement of pin fins resulted in different heat thermal performance. Therisa et al. [8] presented developing model of the heat sink in the Hyoid (U-shaped) PIFHS with configurationally parameterized perforations. Flow types with and without staggered and in-line flow were considered. Based on their findings, they concluded that the hyoid PIFHS outperforms the regular PIFHS in terms of thermal performance. Yang et al. [9] found that an analysis simulation had been developed using the Taguchi technique for pin fin with cooling of air impinging to determine the effects of height and spacing of fin on thermal resistance then to determine the optimal gathering. An adequate inter-fin spacing configuration is revealed to be capable of increasing the Nu. The Nu additions reduce with the increased Re. At high Re, the effects of geometries are ruined.

This is where hollow circular pins offer a different solution by using less material and weight on the structure to be firmer. Research conducted revealed that while using pins with a hollow structure, it was possible to obtain results that would be at par with or even surpass that of solid pins, because of the extensive contact area on pins that is available for heat

exchange. More research should be conducted to investigate the effectiveness of these works at other Reynolds numbers and heat fluxes. Bakhti and Si-Ameur [10] conducted numerical study on the modes of mixed convective for heat transfer between the hollow elliptic fins (perforated) and arrays of solid fin. For the usual arrangement, the characteristics of heat transfer for the novel HSs depend on some critical parameters likes hole position and Reynolds number. Seyf and Layeghi [11] next explored the three-dimensional conjugate heat transfer performance of forced convection heat transfer from an elliptical pin fin heat sink with and without metal foam insertions by employing a model of the same heat transfer. The Darcy–Brinkman–Forchheimer and Navier–Stokes equation is the base of the calculations carried out for the flow field and heat transfer analysis. The analysis discloses the fact that the numerical and the experimental results are coincided with each other by the open-ended heat sink provided with a metal foam insert. It was found that key features of the metal foam’s structure play a crucial part in the flow and heat transfer, with the Nusselt number rising when the porosity and Reynolds number decrease. Maji et al. [12] explored heat transfer enhancement in heat sinks using perforated pin fins in linear and staggered arrangements. Results show that perforated fins have higher heat dissipation rates than solid ones, and staggered arrangements offer better performance. However, pressure drop decreases with perforation size and shape. Optimization analysis and exergy analysis were used to predict optimal fins for maximum heat transfer and minimum pressure loss. The perforated circular pins have an additional set of orifices in the form of perforations that enhances the fluid pathways and thus the convective heat transfer. Scholars said that perforations generate turbulence and interfere with thermal boundary layers in a better manner than solid pins. However, the effect of different sizes and patterns of perforation has not yet determined. Yousfi [13] analyzed forced convection heat transfer and fluid flow characteristics in a pin fin heat sink (PFHS). A new pin design with pyramid fins is proposed, characterized by a ratio of pyramid (ROP) ranging from 0 to 1. The design is validated using COMSOL Multiphysics 5.4 software and found to enhance hydro-thermal performance, with the highest HTPF of 2.1. Hasan et al. [14] investigated heat transfer in a 3-D rectangular microchannel heat sink using CuO/H₂O nanofluid as a coolant. The performance of the microchannel is evaluated using ANSYS Fluent 12.0, focusing on temperature, velocity contours, average Nu, and pressure drop. The thermo-physical properties of the nanofluid are also studied. Results show that using CuO/H₂O nanofluid improves heat transfer by 11%. The study also discusses the effect of the nanofluid concentration on fluid velocity and Reynolds number. Al-Azzawi et al. [15] examined the impact of vertical forced vibration on the free convection heat transfer coefficient (h) of a long-fined aluminum sheet. The test model, with 12 fins, was heated at various tilt angles and frequency ranges. Data analysis revealed a direct connection between the free heat transfer rate and vibration amplitude, and the heat transfer coefficient decreasing when the angle of tilt increased. Heat sinks with pin fin configurations are widely used in electronic cooling due to their better heat transfer coefficients. Khetib et al. [16] focused on the degree of the cooling ability and the productivity of a micro-pin-fin heat sink (MPFHS) using different pin-fin configurations in turbulent, steady, and incompressible flow. This setting was found to be the most efficient by the heat transfer and pressure drop. The result was

that the larger the pin distances, the higher the heat transfer rates were and the pressure drop was higher as well. Jasim et al. [17] evaluated the benefits of pin fins with circular stenosis on their surface by taking into account the heat transition and pressure drop, using this study. The test of the empirical heat sink was done by designing and implementing several circular stenosis, which led to pressure difference less than normal but heat transition to be high when compared to normal fins. It will lead to the heat transfer improvement of about 100% to 223%. The highest heat transfer efficiency, which is equal to 9% compared to the normal fins, is mostly due to the increased surface area and the better heat transition. Al-Abboodi et al. [18] examined a micro heat sink with pin fin and four fin geometries under two layout styles. It describes hydrodynamic and thermal properties in the range of the Reynolds number under constant thermal boundary conditions. The outcomes revealed that a longitude pin fin temperature decreases with an increase of Reynolds number, while a shortening pin fin has the lowest temperature. The ellipse fin structure gives the maximum local heat transfer and the highest Nusselt number. Micro-channel heat sinks were the latest technology in the cooling sector, which provided means for heat to be evacuated through extremely small spaces [19]. They were employed in automotive, air-conditioning and refrigeration industries. The heat sinks made from silicon or copper have micro-channels which force fluid to flow through parallel micro-channels. Nano-fluids can increase the thermal conductivity and fluid convection. It proposed the concept of heat exchange amplification in mini-channels and analyzed recent studies using laminar flow method. Slit circular pins have the advantages of grooves as well as the advantages of perforations. The investigators proved that flow patterns generated by the slits significantly enhance the process of heat transfer. There are many unexplored aspects regarding the influence of the slit dimensions on the flow dynamics.

Oudah et al. [20] has studied the heat transfer efficiency in circular pin-fin heat sinks with notches of varying sizes. It is found that notch size is the main factor determining the efficiency of the heat transfer, particularly for the bigger notches. The notch size of the heat sink at 4 mm shows a 9% growth in Nusselt number and 2.15°C temperature differential compared to heat sinks with solid fins. Every notched heat sink is a plausible choice with the one with the 4 mm size notch having the best performance. In the study conducted by Elmnifi et al. [21], the use of an aluminum heat sink to cool a solar cell is investigated and the effect of microprocessors and integrated circuits on the performance and temperature is examined. The research showed that putting the heat sink into the cell caused the cell's temperature to be reduced gradually and it performed more efficient. The investigation also showed that there is a direct correlation between the number of fins in the heat sink and the heat transfer activity. This might be one of the factors that increase solar power generation efficiency.

This numerical study is conducted on the modes of mixed convective for heat transfer between the hollow elliptic fins (perforated) and arrays of solid fin. For the usual arrangement, the characteristics of heat transfer for the novel HSs depend on some critical parameters likes hole position and Reynolds number.

2. NUMERICAL ANALYSIS

In ANSYS Fluent, steady state CFD detailing was utilized to highlight this issue. Pre-Processing shows how the decided

objective is solved and the computational mesh is created. In the second step, a constant heat flux applied to the matrix base made of aluminum was used using properties of fluid flow with the presence of boundary conditions with an analytical model. Solver will continue to run until the meeting is called. When the solver is done, the results are examined, which is the part of the post that is being prepared.

The Reynolds numbers considered in this investigation (10714.3, 20660, and 32142.86) were chosen to cover a typical operating range for electronic cooling. These values relate to the low to moderate flow rate ranges that are typical for cooling systems of microprocessors, power converters, and LED equipment. Low Reynolds number range is related to natural convection or low-speed forced convection in which little air is utilized to cool the microelectronics. The higher end relates closer to cooling strategies that are more intense with high airflow rates, which are required for performance or compact electrical assemblies. In covering this range, the work is able to ascertain the generality of its findings across different real-world cooling systems; from cooling systems with minimal energy input to those that are more dynamic and efficient. These Reynolds numbers fall within the range that is characteristic of most electronic cooling systems. For example, Reynolds number equal to 10714.3 is suggestive of low speed forced convection, that is often employed in cases where natural convection is inadequate but high-speed fans are either unsuitable due to noise or power considerations. Reynolds number of 20660 depicts a moderate air flow which is suitable for most of the conventional electronics to cool at a stable temperature. Reynolds number of 32142.86 is used in high performance systems where heat has to be dissipated quickly like gaming computers, high power LED strips and telecommunications equipment.

The heat fluxes used for the simulations (3000, 7000, 13000, 18000 and 23000 W/m²) were selected to represent the thermal loads that can be produced by most modern electronic equipment. These values represent the dissipative power of high-performance computing, new-generation telecommunication equipment, and high-brightness LED modules. The lower heat flux value is for low power application or energy efficient devices, while the higher value is for the high-power devices that need proper cooling mechanism to prevent thermal failure and ensure reliable operation. It is thus possible to get a wider range of heat fluxes, which makes the conclusions of the study more versatile, and can be used in both low-power and high-power applications of electronic cooling. These values are the thermal loads created by various electronics in terms of the minimum and maximum values. For instance, 3000 W/m² is used in low power application such as small sensors, or energy efficient microprocessor. 13500 and 18000 W/m² heat flux are observed in high-performance processors, GPU, and high-power LEDs. A heat flux of 7000 W/m² is typical in modern computing and in power electronics where thermal management plays a significant role in system reliability. The highest value of 23000 W/m² is used to define the most modern application, where the thermal dissipation is acutely critical and requires the corresponding cooling.

2.1 Governing equations

The fluid flow is assumed steady state, turbulent, and incompressible. Additionally, the thermos-physical properties of air are assumed to remain constant. Radiant heat transmission and bouncing impacts are irrelevant. According

to the foregoing, the governing equations for the typical k-model are as follows:

2.1.1 Air side

- Continuity equation

$$\frac{\partial u}{\partial x} + \frac{\partial v}{\partial y} + \frac{\partial w}{\partial z} = 0 \quad (1)$$

- X-Momentum equations

$$u \frac{\partial u}{\partial x} + v \frac{\partial u}{\partial y} + w \frac{\partial u}{\partial z} = -\frac{1}{\rho} \frac{\partial p}{\partial x} + \vartheta \left(\frac{\partial^2 u}{\partial x^2} + \frac{\partial^2 u}{\partial y^2} + \frac{\partial^2 u}{\partial z^2} \right) \quad (2)$$

- Y-Momentum equations

$$u \frac{\partial v}{\partial x} + v \frac{\partial v}{\partial y} + w \frac{\partial v}{\partial z} = -\frac{1}{\rho} \frac{\partial p}{\partial y} + \vartheta \left(\frac{\partial^2 v}{\partial x^2} + \frac{\partial^2 v}{\partial y^2} + \frac{\partial^2 v}{\partial z^2} \right) \quad (3)$$

- Z-Momentum equations

$$u \frac{\partial w}{\partial x} + v \frac{\partial w}{\partial y} + w \frac{\partial w}{\partial z} = -\frac{1}{\rho} \frac{\partial p}{\partial z} + \vartheta \left(\frac{\partial^2 w}{\partial x^2} + \frac{\partial^2 w}{\partial y^2} + \frac{\partial^2 w}{\partial z^2} \right) \quad (4)$$

- Energy equation

$$u \frac{\partial T}{\partial x} + v \frac{\partial T}{\partial y} + w \frac{\partial T}{\partial z} = \frac{K_f}{\rho c_p} \frac{\partial p}{\partial x} + \left(\frac{\partial^2 T}{\partial x^2} + \frac{\partial^2 T}{\partial y^2} + \frac{\partial^2 T}{\partial z^2} \right) \quad (5)$$

2.1.2 Solid side

$$K_s \left(\frac{\partial^2 T}{\partial x^2} + \frac{\partial^2 T}{\partial y^2} + \frac{\partial^2 T}{\partial z^2} \right) + \dot{q} = 0 \quad (6)$$

where, K_f and K_s denote the thermal conductivity of the fluid and heat sink respectively, T indicates the temperature in the heat sink, and w , v , and u indicate the velocity components. While \dot{q} indicates the heat generated per unit volume.

2.2 Domain and BCs

Figure 1 illustrates the distribution of the heat sink's meshes and calculation domain for the enclosure and the heat sink pin fin. The inlet velocity, outlet pressure, and wall conditions, as well as symmetry BCs in the computational domain, were applied. The mentioned boundary conditions which are shown in Figure 1.

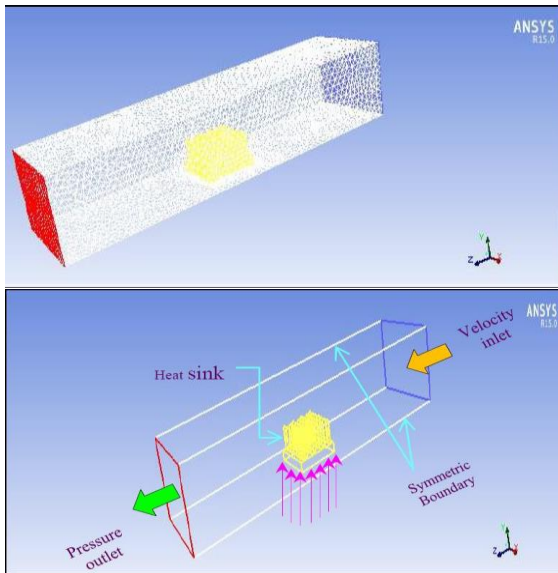


Figure 1. Distribution of the heat sink's meshes and calculation domain

The boundary conditions were defined as follows:

Inlet boundary: Inlet with uniform velocity in the centerline with velocities corresponding to $Re=10714.3$ to 432142.86.

Outlet boundary: Flow boundary condition with the atmospheric pressure of $P_{out}=101325$ Pa.

Wall boundary: Non-adiabatic boundary condition on all the rigid boundaries. The bottom of the heat sink received a heat flux ranging from 3000 to 23000 W/m².

Inlet

$$P=P_{in}, T=T_{in}=300 \text{ K}, W=V_{in}, u=v=0$$

Outlet

$$P=P_{out}, u=v=0, \frac{\partial T}{\partial z} = 0$$

Walls

$$u=v=w=0, \frac{\partial T}{\partial x} = \frac{\partial T}{\partial y} = 0$$

Heated wall

$$u=v=w=0, q_w = \frac{\partial T}{\partial x}$$

The fluid used in the simulations was air, with the following properties assumed to be constant:

• Density (ρ): 1.225 kg/m³

• Dynamic viscosity (μ): 1.7894×10⁻⁵ kg·m/s

• Thermal conductivity (k): It is noteworthy that he has no role in the preparation of the dishes and does not even help cook them to the extent that a non-cooking spouse might in a typical home-cooking scene: 0.0257 W/m·K

• Specific heat capacity (cp): 1006 J kg⁻¹K⁻¹

This assumption is made due to the fact differing from the heat sink operational temperatures are not very large and therefore do not affect the properties of the fluid. The simulations used the k-ε turbulence model including the realizable k-ε model with improved near-wall treatment. This variant was chosen because it is more stable and provides better solutions to calculate complicated flow fields in heat transfer problems. Turbulence boundary conditions were specified as follows:

• Turbulence intensity at the inlet: 5 percent

• Turbulence length scale at the inlet: There is a nil probability that women are exploited in the channel 7 times the hydraulic diameter

The computational domain was discretized using a block structured grid with hexahedral cells in the core region and prismatic/tetrahedral cells in the vicinity of the walls and pin surfaces to capture the boundary layer effects. The given mesh sizes were decided with the help of the mesh independency study, where the density of the mesh was changed and the difference in key parameters was observed. The medium mesh was chosen for the last simulations since it offered a proper balance between precision and calculation time. To address near-wall treatment, special attention was paid to maintain a dimensionless wall distance, y^+ , below unity for the first cell layer in interaction with the walls. The following discretization schemes were used for the various terms in the governing equations:

• Second-order upwind scheme is a type of finite volume

method that involves upwind differencing of the fluxes.

- Central differencing scheme also called centred differencing scheme.

- Pressure-velocity coupling: SIMPLE (Semi-Implicit Method for Pressure Linked Equations).

- A scheme that is implicit with time step guaranteeing that the Courant number is less than unity.

Convergence was monitored through the residuals of the governing equations, with the following criteria used to determine convergence:

- Continuity: Any value of the residuals less than 10^{-3} .

- Momentum: The residual should be less than 10^{-3} .

- Energy: The permissible residual values have been reached and do not exceed 10^{-6} .

- Turbulence quantities (k and ϵ): The values of residuals should be less than 10^{-4} .

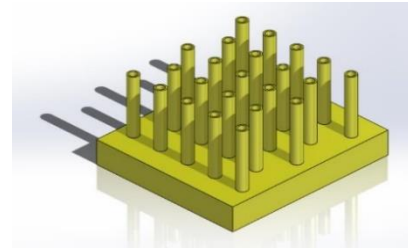
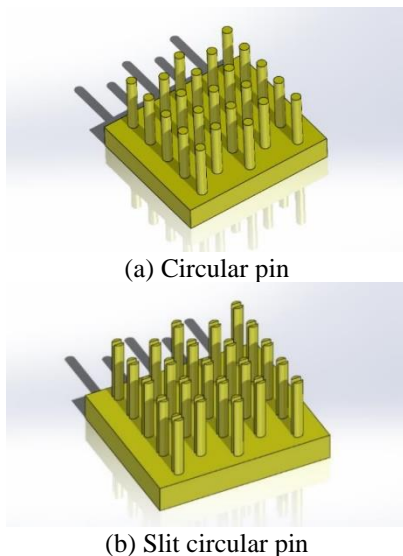
A fully developed velocity profile at the inlet was defined and velocities for the inlet varied according to the Reynolds numbers investigated in the work. The inlet temperature was fixed to a certain value of T_{in} as the value of x changed.

An outflow BC was applied, which means that the flow has to exit the computational domain without any dramatic changes in velocity. The outlet pressure was set to atmospheric pressure.

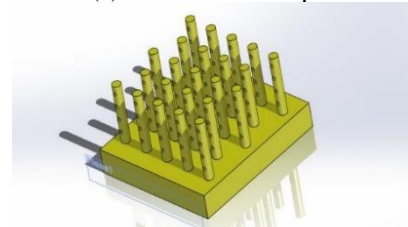
For the completely solid walls, including the heat sink base and pin surfaces, the no-slip condition was applied. The heat flux used in this research was applied to the base of the heat sink in accordance to the study objectives.

2.3 Model section description

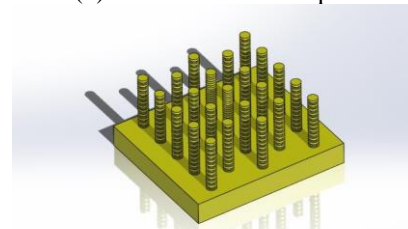
To improve the performance of the pin-fin, different shapes are designed for the fins in this study; five different aluminum PIFHSs were drawn using solid work software. The closure cross-section area is (150 mm×200 mm) and a closure length of 800 mm. The outside diameter of all pin fins is 7 mm with the same height by 45 mm and the total number of heat sink pin fins is 23. The length and thickness of the base plate are 114 mm and 18.5 mm respectively. The pin fin arrays which are staggered separated by an equal distance streamwise and spanwise directions ($ST=SL=20$ mm). The configurations of all pin fin heat sink (PIFHSs) are shown in Figure 2. Where there are five different shapes of pin fins that have the same hydraulic diameter: circular pin, circular pin with circumferential groove, hollow circular pin, perforated circular pin, and slit circular pin.



(c) Hollow circular pin



(d) Perforated circular pin



(e) Circular pin with circumferential groove

Figure 2. The pin fin configurations

Mesh generation: The computational domain was meshed using an unstructured mesh but with more grid points near the pin and heat sink surfaces to account for the boundary layer.

A comprehensive mesh independence study was conducted:

Mesh types: Structured mesh approximately wall and unstructured mesh far from the wall in the bulk fluid.

Mesh refinement: A mesh independence study was performed by gradually reducing the mesh and analyzing how temperature distribution is affected.

Results: The final mesh was determined according to the compromise between the computational time and precision: further increase in the density did not affect the result largely. For instance, beyond certain mesh density, some of the finite element approximations cannot be used.

3. NUMERICAL RESULTS

The results are limited to the distribution of static temperatures in heat sinks on a local scale. Figure 3 depicts the filled contour of the heat sink's temperature with constant heat flux (23000 W/m^2) and constant air velocity (3 m/s) in a wind tunnel for different pin fin shapes. Extreme temperatures are reported for all heat sink pin fin shapes (PIFHS) of the base plate. In general, the base temperature of all pin fin shapes is higher than at the top surface suggests that air is cooling the top surface. The centers of all heat sink pin fin shapes forms the hottest areas due to higher levels of heat transmission between the air and the aluminum near the heat source on the bottom surface. The lowest base plate temperatures measured for circular pins were with circumferential grooves.

To complement the quantitative results, temperature plots obtained from the simulations and depicted in the figure have been employed to depict the thermal characteristics of various

pin layouts. The temperature distribution of the grooved circular pin configuration indicates the variation of temperature in the heat sink. The areas of higher temperature are depicted in red color and cooler areas in blue color. This visualization is useful in analyzing the thermal efficiency or lack of it in the heat sink design.

Perforated circular pins: Explain why the highest Nusselt numbers and heat transfer coefficients occur at all Re due to turbulence and surface area.

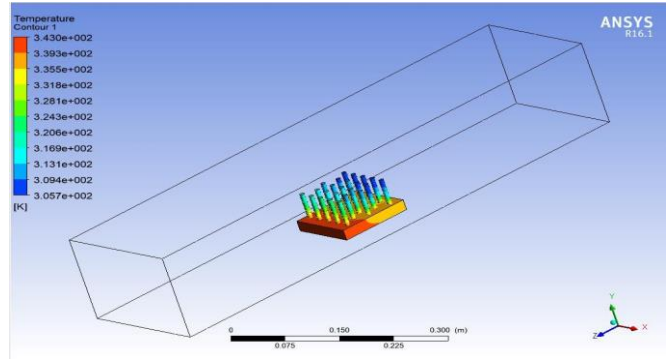
Grooved circular pins: Increase turbulence of the flow to increase mixing and thus obtain better convective heat transfer.

Hollow circular pins: Perform slightly under the solid pins but offer a good combination of performance and the amount of material used.

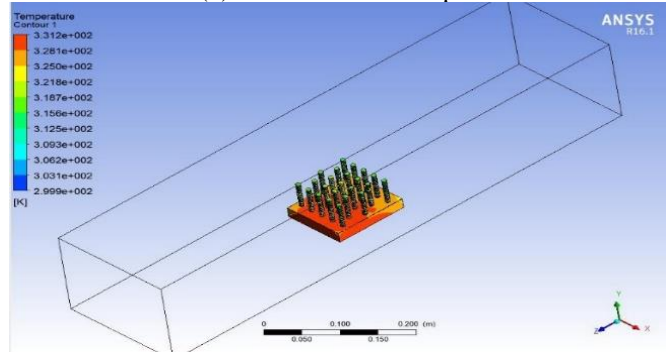
Slit circular pins: Also increase the flow disruption and increase the turbulence for the enhancement of heat transfer.

Grooves, perforations, and slits led to the higher pressure drops hence higher flow resistances. The pressure drop was the highest for the perforated circular pins while grooved and slit pins were the second highest. Among the modified configurations, the pressure drop was least in the hollow circular pins but with moderate performance.

Figure 4 shows influence of heat flux on Nu with constant Reynold number (Re=20660) for all pin fin heat sink shapes. This figure reveals that Nu increases with increasing heat flux. The increment in the Nu may due to an increase in the amount of heat transfer. For perforated PIFHS, the Nu is 491.569 and 760.294 at 3000 and 23000 W/m², respectively.

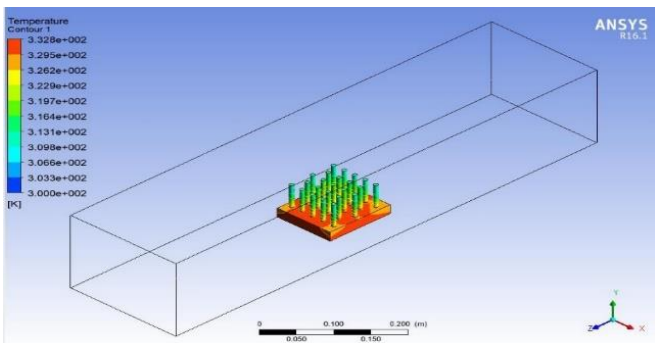


(d) Perforated circular pin

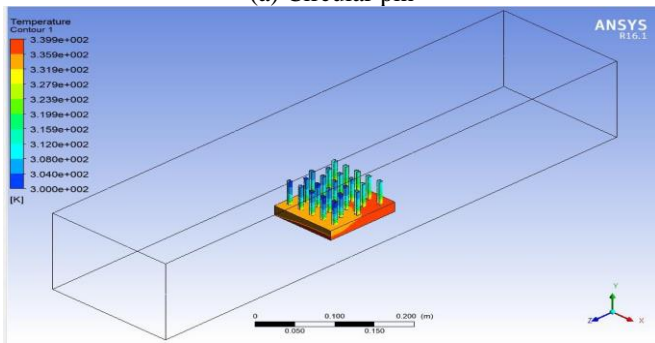


(e) Circular pin with circumferential groove

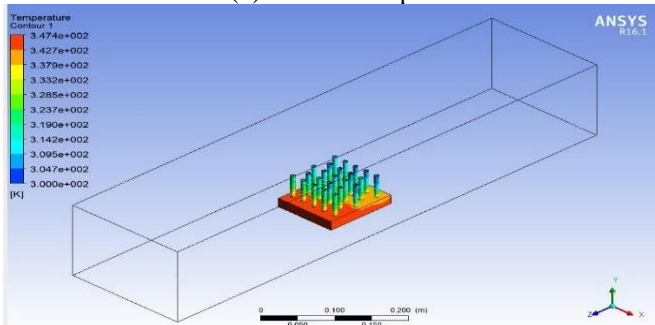
Figure 3. Temperature contour of the five-pin fin heat sink shape (a), (b), (c), (d), (e)



(a) Circular pin



(b) Slit circular pin



(c) Hollow circular pin

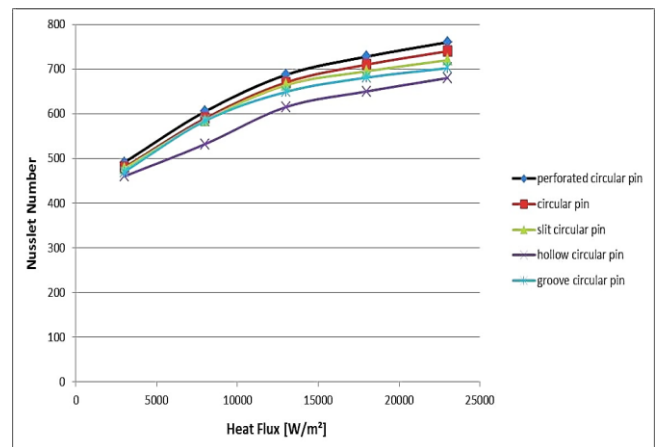


Figure 4. Distribution of Nu with heat flux

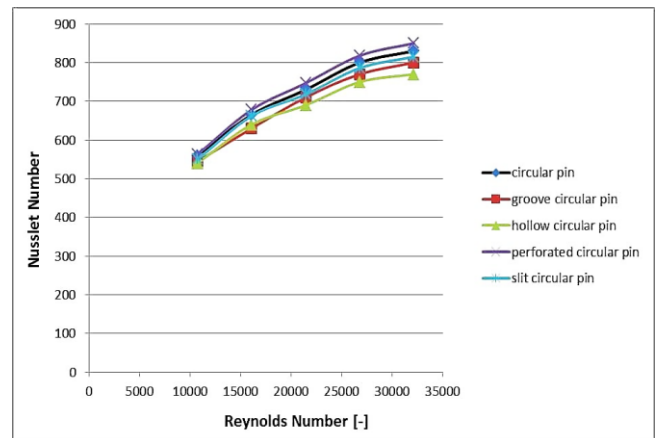


Figure 5. Distribution of Nu with Re

Figure 5 shows influence of Re on Nu with a constant heat flux (23000 W/m²). The Nu increases as the Re increases for each pin shape. It is plain to see that the increment in the Nu because of the increment in heat transfer generated by the increasing in airflow rate. For the perforated pin fin PIFHS, the Reynolds numbers are 10714.3 and 32142.86, respectively, and the Nusselt numbers are 563.0634 and 850.1398.

Concerning the comment to include more quantitative analysis, it will develop a detailed explanation of the heat transfer coefficient, the Nusselt number, and the pressure drop from the given figure and data. This will involve an explanation of the activities that will be carried out to arrive at these parameters and the meaning of these parameters.

From Figure 5, it is shown that the Nusselt number (Nu) increases with the increase in Reynolds number (Re) and pin configuration in the heat sink. The analysis focuses on five types of pin configurations: First, there is circular pins; grooved circular pins; hollow circular pins; perforated circular pin; and last is slit circular pin. All the pin configurations show a rising trend of the Nusselt number, a dimensionless parameter related to heat transfer efficiency, with the Reynolds number. This is quite understandable bearing in mind that there is a general expectation that higher Reynolds numbers, implying higher flow rates, will improve convective heat transfer.

Circular pin: For a Reynolds number of 5000 the Nusselt number is roughly 600.

With the increase in Reynolds numbers, the Nusselt number increases and reaches 850 at Re=30000.

Grooved circular pin: Shows the same trend as Re, and reaches a value of around 610 at Re=5000. Rises to about 860 at Re=30000.

Hollow circular pin: Commences at a relatively lower Nusselt number of 590 when the Reynolds number is 5000. Rises up to around 830 at Re=30000.

Perforated circular pin: Reveals better performance at lower Re values and has Nusselt number of 630 at Re=5000. The highest Nusselt number of approximately 880 is attained among the configurations at Re=30000.

Slit circular pin: Starts at 620 when Re=5000. Rises to a maximum of about 870 at Re=30000.

All the configurations exhibit a rise in the Nusselt number with Reynolds number, this is an implication that convective heat transfer is improved with increased flow rates.

Perforated circular pins: These always exhibit the highest Nusselt numbers proving that more turbulence and surface area for heat transfer is better.

Circular pin shapes with grooves and slits function similarly, with somewhat lower Nusselt numbers than perforated pins but still greater than hollow pins.

Hollow circular pins: These have the lowest Nusselt values of all the adjusted configurations, which suggests that heat transfer is less effective. This is probably because there is less surface area available for heat exchange.

Pins with grooves: The grooves probably improve heat transfer by increasing turbulence. When contrasted with standard round pins, this leads to greater Nusselt numbers.

Hollow pins: Lower heat transfer rates could result from the hollow structure's potential to reduce surface area.

Perforated pins: By drastically altering the flow, the holes increase turbulence, which improves heat transmission.

Slit pins: By obstructing the flow and increasing turbulence, the slits function similarly to perforations in terms of improving heat.

The thermal performance of heat sinks can be greatly impacted by the pin arrangement that is used. Because of their improved heat transmission characteristics, perforated circular pins are advised for applications needing significant heat dissipation. Nevertheless, there may be a trade-off in the form of possibly larger pressure drops, which the cooling system design must take into account.

The significance of geometric alterations in improving heat transfer performance is brought to light by the analysis of the Nusselt number distribution with Reynolds number for various pin arrangements. Hollow circular pins might be more appropriate for situations where a smaller pressure drop is a top concern, but perforated and grooved circular pins show the most potential for those needing effective thermal management. Additional quantitative evaluation of variables such as pressure decrease and comprehensive statistical analysis.

For all pin fin heat sinks, the variation of the (h) with heat flux with a constant Reynolds number (Re=20660) is shown in Figure 6. This figure reveals that the increase of (h) by increasing the heat flux. In addition, it is found that the perforated circular pin has the greatest heat transfer coefficient comparing with other types due to its larger wetted surface area.

The heat transfer coefficient for various PIFHSs compared to various Reynolds numbers for heat flux=23000 W/m² is shown in Figure 7. In general, the (h) increases with increasing the Re. The increase of (h) with Re is may due to increasing the amount of air, increasing of flow capability of heat released which in turn result in an improved of (h) in PIFHSs. It is also demonstrated that the perforated circular pin achieves the highest heat transfer coefficient due to greater heat removal than other types.

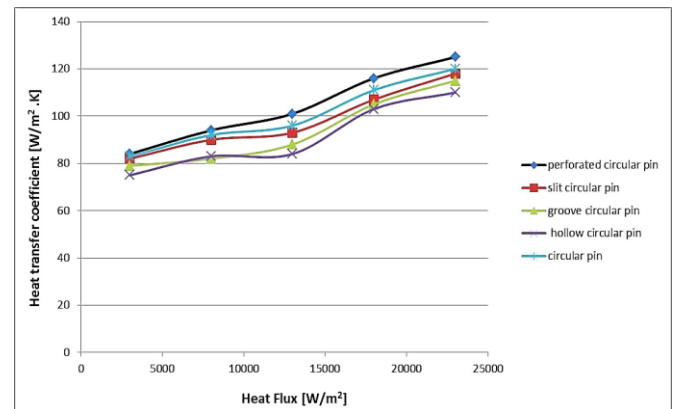


Figure 6. The variation of (h) with heat flux

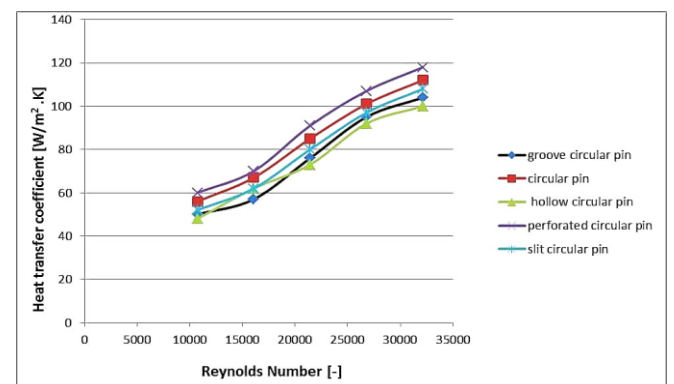


Figure 7. The distribution of (h) with Reynold number

The variations in the observed performance are thus due to the differences in geometry that alter the flow field and heat transfer characteristics as observed in the case of the various pin arrangements. The grooves help in increasing the turbulence in the flow which in turn increases the mixing and thus the convective heat transfer as is evident from the 2.67% increase in Nu. Although this lessens the amount of material used in the design, the hollow structure of the fins minimizes the heat transfer area slightly and gives a Nu of 2% less than the flat fins. Thus, perforations affect the boundary layer greatly, increasing turbulence and surface area that results to the highest improvement in Nu by 5.33%. The slits promote flow disturbance and raise the level of turbulence and thus, the Nu increases by 2%.

4. CONCLUSIONS

This paper focused on the thermal characteristics of different circular pin arrangements in heat sinks through computational analysis in ANSYS Fluent. The configurations were basic round head pins, knurled round head pins, plain round head pins, punched round head pins and slotted round head pins. The numerical performance of turbulent forced convection of various pin-fin shapes has been examined in the current paper. Thermal performance characteristics of pin fin heat sinks were conducted by examining the geometrical and operational parameters influences. The most essential conclusions can be stated by assessing the current work outcomes as follows:

1. A perforated circular pin has a better heat transfer path than conventional circular pin fin.
2. The Reynold number of the air which is incoming has an effect on the Nusselt number with constant heat flux.
3. When compared to all circular pin-fins arrays, a perforated circular pins array has a larger Nusselt number.
4. The lowest reported base plate temperatures for circumferential groove circular pins.

The key findings and novel insights from this study are summarized as follows:

(1) In the case of the configurations investigated, circular pins with perforations had the highest Nusselt numbers as the Reynolds number was varied, thus portraying the best heat transfer rates. Grooved and slit circular pins also revealed that it has better heat transfer coefficients than the standard circular pins due to the turbulence and improved surface area.

(2) The grooves, perforations and slits made on the heat sink fins helped in increasing the pressure drop across the heat sink. Hollow circular pins, though used less material, had a fair rise in pressure drop, thus providing a conclusive trade-off between performance and economy.

(3) The Reynolds numbers as well as the heat fluxes considered in this investigation were chosen to represent realistic operating conditions in electronic cooling systems. The conclusions show that changing the positions of the pins can improve the heat sink performance considerably; hence, they are useful for real-world scenarios.

(4) The work presents different advanced configurations of the pins, and it is revealed that both perforated and slit pins can improve heat transfer coefficient. These findings aid in the enhancement of heat sink designs for effective heat dissipation in electric equipment.

(5) More work should be done to investigate the application of these new pin configurations in the long-term stability and

mass production. It would be valuable to have experimental validation of the numerical results obtained in the study. Researching the efficiency of these configurations under different heat flux rates and with other fluids might provide more information on their usability in various situations.

REFERENCES

- [1] Li, H.Y., Chao, S.M., Tsai, G.L. (2005). Thermal performance measurement of heat sinks with confined impinging jet by infrared thermography. *International Journal of Heat and Mass Transfer*, 48(25-26): 5386-5394. <https://doi.org/10.1016/j.ijheatmasstransfer.2005.07.007>
- [2] Khan, W.A., Culham, J.R., Yovanovich, M.M. (2008). Modeling of cylindrical pin-fin heat sinks for electronic packaging. *IEEE Transactions on Components and Packaging Technologies*, 31(3): 536-545. <https://doi.org/10.1109/TCAPT.2008.2002554>
- [3] Muhammad, E.H. (2015). A comparison of the heat transfer performance of a hexagonal pin fin with other types of pin fin heat sinks. *International Journal of Science and Research*, 4(9): 1781-1789.
- [4] Arefin, A.M.E. (2016). Thermal analysis of modified pin fin heat sink for natural convection. In 2016 5th International Conference on Informatics, Electronics and Vision (ICIEV), Dhaka, Bangladesh, pp. 1-5. <https://doi.org/10.1109/ICIEV.2016.7759986>
- [5] Muthukumarn, R., Rathnasamy, R., Karthikeyan, R., Nadu, T., Tunnel, W. (2016). Experimental study of performance of pin fin heat sink under forced convection. *International Journal of Mechanical Engineering and Information Technology*, 4(10): 1791-1796.
- [6] Manikandan, C., Pachaiyappan, S. (2016). Transient thermal simulation of perforated drop-shaped pin fin array in staggered arrangement. *International Journal of Innovative Research in Science, Engineering and Technology*, 5(2): 2193-2202.
- [7] Annuar, K.A.M., Ismail, F.S., Harun, M.H., Halim, M.F.M.A. (2015). Inline pin fin heat sink model and thermal performance analysis for central processing unit. *Proceedings of Mechanical Engineering Research Day*, 2015: 35-36.
- [8] Therisa, T., Srinivas, B., Ramakrishna, A. (2014). Analysis of hyoid structured and perforated pin fin heat sink in inline and staggered flow. *International Journal of Science Engineering and Advance Technology*, 2(4): 125-130.
- [9] Yang, Y.T., Peng, H.S., Hsu, H.T. (2013). Numerical optimization of pin-fin heat sink with forced cooling. *International Journal of Electronics and Communication Engineering*, 7(7): 884-891.
- [10] Bakhti, F.Z., Si-Ameur, M. (2016). Numerical study of cooling enhancement: Heat sink with hollow perforated elliptic pin fins. *Computational Thermal Sciences: An International Journal*, 8(5): 409-428. <https://doi.org/10.1615/ComputThermalScien.2016017354>
- [11] Seyf, H.R., Layeghi, M. (2010). Numerical analysis of convective heat transfer from an elliptic pin fin heat sink with and without metal foam insert. *ASME Journal of Heat and Mass Transfer*, 132(7): 071401. <https://doi.org/10.1115/1.4000951>

- [12] Maji, A., Bhanja, D., Patowari, P.K. (2017). Numerical investigation on heat transfer enhancement of heat sink using perforated pin fins with inline and staggered arrangement. *Applied Thermal Engineering*, 125: 596-616. <https://doi.org/10.1016/j.applthermaleng.2017.07.053>
- [13] Yousfi, A. (2019). Effects of a pyramidal pin fins on CPU heat sink performances. *Journal of Advanced Research in Fluid Mechanics and Thermal Sciences*, 63(2): 260-273.
- [14] Hasan, W.K., Kalash, A.R., Hussien, H.M., Habeeb, L.J. (2020). Numerical Investigation of Nanofluid in a Rectangular Microchannel Heat Sink. *Journal of Mechanical Engineering Research and Developments*, 43(6): 404-417.
- [15] Al-Azzawi, M.M., Hussain, H.M., Habeeb, L.J. (2020). An experimental study on the influence of forced vibration on longitudinal fins heat sink subjected to free convection heat transfer. *Journal of Mechanical Engineering Research and Developments*, 43(7): 326-339.
- [16] Khetib, Y., Sedraoui, K., Gari, A. (2021). Numerical study of the effects of pin geometry and configuration in micro-pin-fin heat sinks for turbulent flows. *Case Studies in Thermal Engineering*, 27: 101243. <https://doi.org/10.1016/j.csite.2021.101243>
- [17] Jasim, H.A., Kassim, M.S., Hussain, A.A., Habeeb, L.J. (2021). Investigation of heat transfer enhancement for different shapes pin-fin heatsink. *Journal of Mechanical Engineering Research and Developments*, 44(3): 75-89.
- [18] Al-Abboodi, N.K., Khalaf, K.A., Ridha, H., Al-Azawy, M.G. (2022). Thermal and flow analysis of different shaped pin fins for improved heat transfer rate. *International Journal of Heat and Technology*, 40(1): 201-210. <https://doi.org/10.18280/ijht.400124>
- [19] Hadi, J.M., Abdullah, A.R., Majel, B.M., Habeeb, L.J. (2023). Heat transfer augmentation in a micro-channel heat sink technique under different coolant flow: A comprehensive review of the recent literature. *AIP Conference Proceedings*, 2839(1): 020003. <https://doi.org/10.1063/5.0168939>
- [20] Oudah, M.H., Ajlan, W.A., Hussien, W.Q., Yasser, Z.K. (2023). Effect of notched pin fin heat sink on the heat transfer performance: Numerical study. *Mathematical Modelling of Engineering Problems*, 10(3): 985-992. <https://doi.org/10.18280/mmep.100332>
- [21] Elmnifi, M., Mansur, A.N., Hassan, A.K., Abdullah, A. R., Ayed, S.K., Majidi, H.S., Habeeb, L.J. (2024). Experimental and simulation study for improving the solar cell efficiency by using aluminum heat sinks. *Proceedings on Engineering*, 6(1): 161-170. <https://doi.org/10.24874/PES06.01.018>